THREE DIMENSIONAL VIEW REGISTRATION BY A FREQUENCY DOMAIN TECHNIQUE

G.M. Cortelazzo, G. Doretto, L. Lucchese, S. Totaro
Department of Electronics and Informatics
University of Padova
Via Gradenigo 6/A, 35131, Padova, ITALY
Tel: +39-49-827 7500; Fax: +39-49-827 7699
e-mail: {corte,doretto,lulaluc,tost}@dei.unipd.it

ABSTRACT

This work presents the algorithmic variations of a 3-D motion estimation method which make it suitable to 3-D view registration. Important characteristics are that the method is suitable for unsupervised 3-D registration and that texture information can be incorporated with beneficial effects on the overall 3-D registration performance. A peculiarity of the method is that it operates in the frequency domain.

1 INTRODUCTION

Textured 3-D models of real objects are obtained by various tasks: i) the aquisition of partial 3-D scans of the object; ii) their geometric alignement or registration, which is typically done by the ICP algorithm and its extensions [1, 2, 3]; iii) the surface modelization of the 3-D data by polygonal meshes; iv) the registration of the object's texture with the corresponding structure.

This work reports on a new method for solving step ii) and it presents some variations to the original algorithmic idea [4], imposed by the nature of what was found to affect the algorithm as noise with 3-D scans. This disturbance is rather difficult to model as it may be due, besides to the inevitable aquisition noise, to occlusions or asymmetries of the partial scans. The problems of the various causes of noise on the algorithm of [4] have been clearly assessed through experimentation, and effective cures against are presented.

2 PROBLEM STATEMENT

Let $s_1(\mathbf{x})$, $\mathbf{x} \in I\!R^3$, be the data of the textured surface of a 3-D object and let $s_2(\mathbf{x})$ be a rigidly translated and rotated version of $s_1(\mathbf{x})$, i.e.

$$s_2(\mathbf{x}) = s_1(R^{-1}\mathbf{x} - \mathbf{t}) \,. \tag{1}$$

According to (1) $s_2(\mathbf{x})$ is first translated by the vector $\mathbf{t} \in I\!R^3$ and then rotated by the matrix[1] $R \in SO(3)$.

Data of this kind, in the view registration problem, may be obtained from the common part of two partially overlapped 3-D scans of an object.

[1] $SO(3) = \{R \in I\!R^{3\times 3}, R^{-1} = R^T, \det(R) = +1\}$ is the group of the 3×3 special orthogonal matrices.

We build 3-D companion solids, denoted as $\ell_i(\mathbf{x})$, of 3-D scans by convolving the 3-D textured surfaces $s_i(\mathbf{x})$ with a small sphere centered around the origin. With the data we used, which typically were matrices $128 \times 128 \times 128$, a sphere with 9 pixels diameter was found to be a good choice. The purpose of this convolution is to create small weighted solid regions around 3-D textured surface $s_i(\mathbf{x})$, with weight decreasing with the distance from $s_i(\mathbf{x})$. In this way solids $\ell_i(\mathbf{x})$ ideally maintain the same spatial information of the 3-D surfaces $s_i(\mathbf{x})$, including that of the texture, without creating the mathematical difficulties given in the Fourier domain by the impulsive supports of $s_i(\mathbf{x})$. Fig.1-(a) shows a view of the range data surface $s_1(\mathbf{x})$ (namely the file `JET1` of [7]) and Fig.1-(b) a view of its companion solids $\ell_1(\mathbf{x})$.

Denote as

$$\mathcal{L}_i(\mathbf{k}) \doteq \mathcal{F}[\ell_i(\mathbf{x}) \mid \mathbf{k}] = \iiint_{-\infty}^{+\infty} \ell_i(\mathbf{x}) e^{-j\,2\pi \mathbf{k}^T \mathbf{x}}\, d\mathbf{x} \,, \tag{2}$$

$$i = 1, 2 \quad , \quad \mathbf{k} = \begin{bmatrix} k_x & k_y & k_z \end{bmatrix}^T \,,$$

the 3-D cartesian Fourier transform of $\ell_i(\mathbf{x}), i = 1, 2$; it is straightforward to prove that (1) implies that the two transforms are related as

$$\mathcal{L}_2(\mathbf{k}) = \mathcal{L}_1(R^{-1}\mathbf{k}) e^{-j\,2\pi \mathbf{k}^T R \mathbf{t}} \tag{3}$$

therefore their magnitudes are related as

$$|\mathcal{L}_2(\mathbf{k})| = |\mathcal{L}_1(R^{-1}\mathbf{k})| \,. \tag{4}$$

The algorithm of [4] uses relationship (4) in order to determine R in the frequency domain. After estimating R it also determines $\mathbf{t}$, as the two problems can be nicely decoupled in the frequency domain [4]. In the following we will motivate the variations from the algorithm of [4] found beneficial with actual 3-D scans.

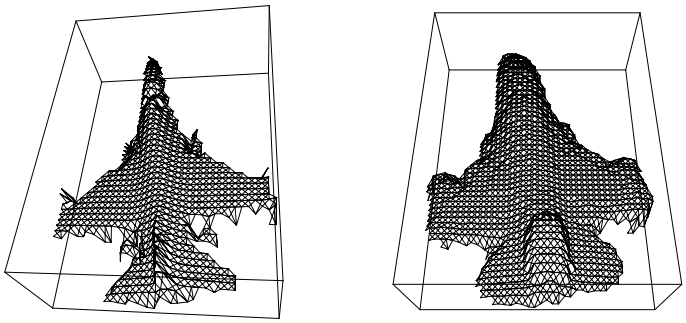

(a) (b)

Figure 1: (a) Example of $s_i(\mathbf{x})$: range image `JET1` of [7]; (b) its companion solid.

3 ALGORITHMIC CHANGES

3.1 Estimate of the rotational axis ω

The algorithm of [4] searches for the locus of null values in the difference function

$$\mathcal{Q}(\mathbf{k}) \doteq \left| \frac{|\mathcal{L}_1(\mathbf{k})|}{\mathcal{L}_1(\mathbf{0})} - \frac{|\mathcal{L}_2(\mathbf{k})|}{\mathcal{L}_2(\mathbf{0})} \right| = \left| \frac{|\mathcal{L}_1(\mathbf{k})|}{\mathcal{L}_1(\mathbf{0})} - \frac{\left|\mathcal{L}_1(R^{-1}\mathbf{k})\right|}{\mathcal{L}_1(\mathbf{0})} \right|, \tag{5}$$

since from (5) it is clear that $\mathcal{Q}(\mathbf{k}) = 0$ if $R^{-1}\mathbf{k} = \mathbf{k}$ which is equivalent to $R\mathbf{k} = \mathbf{k}$. It can be straightforwardly proved that the rotational matrix R possesses eigenvalues $\lambda_1 = 1$, $\lambda_2 = e^{j\psi}$ and $\lambda_3 = e^{-j\psi}$, where ψ is the angular shift around the rotation axis corresponding to R. If ω denotes the unit vector pointing towards the same direction of the rotation axis, it can be proved that ω has the following properties: i) it is the eigenvector associated to $\lambda_1 = 1$ (therefore it satisfies $R\mathbf{k} = \mathbf{k}$); ii) it is the only real eigenvector of R. In other words the locus $\mathcal{Q}(\mathbf{k}) = 0$ includes a line through ω. For objects without special symmetries (as natural objects typically are) this property of the function $\mathcal{Q}(\mathbf{k})$ can be exploited in order to determine the versor ω.

Since $\mathcal{Q}(\mathbf{k})$ can be small both because $|\mathcal{L}_1(\mathbf{k})|/\mathcal{L}_1(\mathbf{0})$ and $|\mathcal{L}_2(\mathbf{k})|/\mathcal{L}_2(\mathbf{0})$ are nearly equal or because they are both rather small, but nonetheless different, it was found beneficial to replace it with

$$\mathcal{Q}'(\mathbf{k}) \doteq \left| \left| \log_{10} \frac{|\mathcal{L}_1(\mathbf{k})|}{\mathcal{L}_1(\mathbf{0})} \right|^{\frac{1}{4}} - \left| \log_{10} \frac{|\mathcal{L}_2(\mathbf{k})|}{\mathcal{L}_2(\mathbf{0})} \right|^{\frac{1}{4}} \right| . \tag{6}$$

The impact of the frequency regions associated to low dynamic range values of $|\mathcal{L}_1(\mathbf{k})|/\mathcal{L}_1(\mathbf{0})$ and $|\mathcal{L}_2(\mathbf{k})|/\mathcal{L}_2(\mathbf{0})$ on locus $\mathcal{Q}'(\mathbf{k}) = 0$ is not as pronaunced as in locus $\mathcal{Q}(\mathbf{k}) = 0$, therefore the use of $\mathcal{Q}'(\mathbf{k})$ greatly simplifies the search for the rotational axis. This 3-D problem in [4] is conveniently turned into a 2-D one by the following procedure:

1) express $\mathcal{Q}'(k_x, k_y, k_z)$ in spherical coordinates as $\overline{\mathcal{Q}}(k_\rho, k_\varphi, k_\theta)$; notice that this function can be represented only in a hemisphere because of the hermitian symmetry of the Fourier transform;

2) compute the radial projection of $\overline{\mathcal{Q}}(k_\rho, k_\varphi, k_\theta)$ as

$$\mathcal{P}(k_\varphi, k_\theta) \doteq \int_0^\infty \overline{\mathcal{Q}}(k_\rho, k_\varphi, k_\theta)\, dk_\rho \; ; \tag{7}$$

3) compute the angular coordinates of ω in spherical representation as

$$(\varphi, \theta) \doteq \arg \min_{k_\varphi, k_\theta} [\mathcal{P}(k_\varphi, k_\theta)] \; , \tag{8}$$

since, from the inclusion of ω within the locus $\mathcal{Q}'(\mathbf{k}) = 0$, $\mathcal{P}(k_\varphi, k_\theta) \geq 0$ with $\mathcal{P}(\varphi, \theta) = 0$;

4) define ω the versor of the direction (φ, θ).

Projection along axis k_ρ, in practice, is very sensitive to discretization, inevitable with numerical implementations of (7), and the occurance of spurious local minima is not infrequent.

The following variations to the above procedure based on $\mathcal{Q}'(\mathbf{k})$ were found beneficial. Since $\mathcal{Q}'(\mathbf{k})$ has considerably more high frequency content than $\mathcal{Q}(\mathbf{k})$ by definition, it is appropriate to low-pass filter it by $H(k_\rho, k_\varphi, k_\theta)$ in such a way to retain not more than the 70% of its low-frequency energy: let's call $\overline{\mathcal{Q}}' = H\overline{\mathcal{Q}}$. Instead of projecting $\overline{\mathcal{Q}}'(k_\rho, k_\varphi, k_\theta)$ along axis k_ρ by (7) in order to obtain a 2-D surface to search for minima, we replace steps 2′) and 3′) by the following ones:

2′) compute

$$\mathcal{P}'(k_\varphi, k_\theta) \doteq \sum_{k_\rho \geq 0} \min_{(k'_\varphi, k'_\theta) \in W(k_\rho, k_\varphi, k_\theta)} \overline{\mathcal{Q}}'(k_\rho, k'_\varphi, k'_\theta) \; ; \tag{9}$$

3′) compute

$$(\hat{\varphi}, \hat{\theta}) \doteq \arg \min_{k_\varphi, k_\theta} [\mathcal{P}'(k_\varphi, k_\theta)] \; . \tag{10}$$

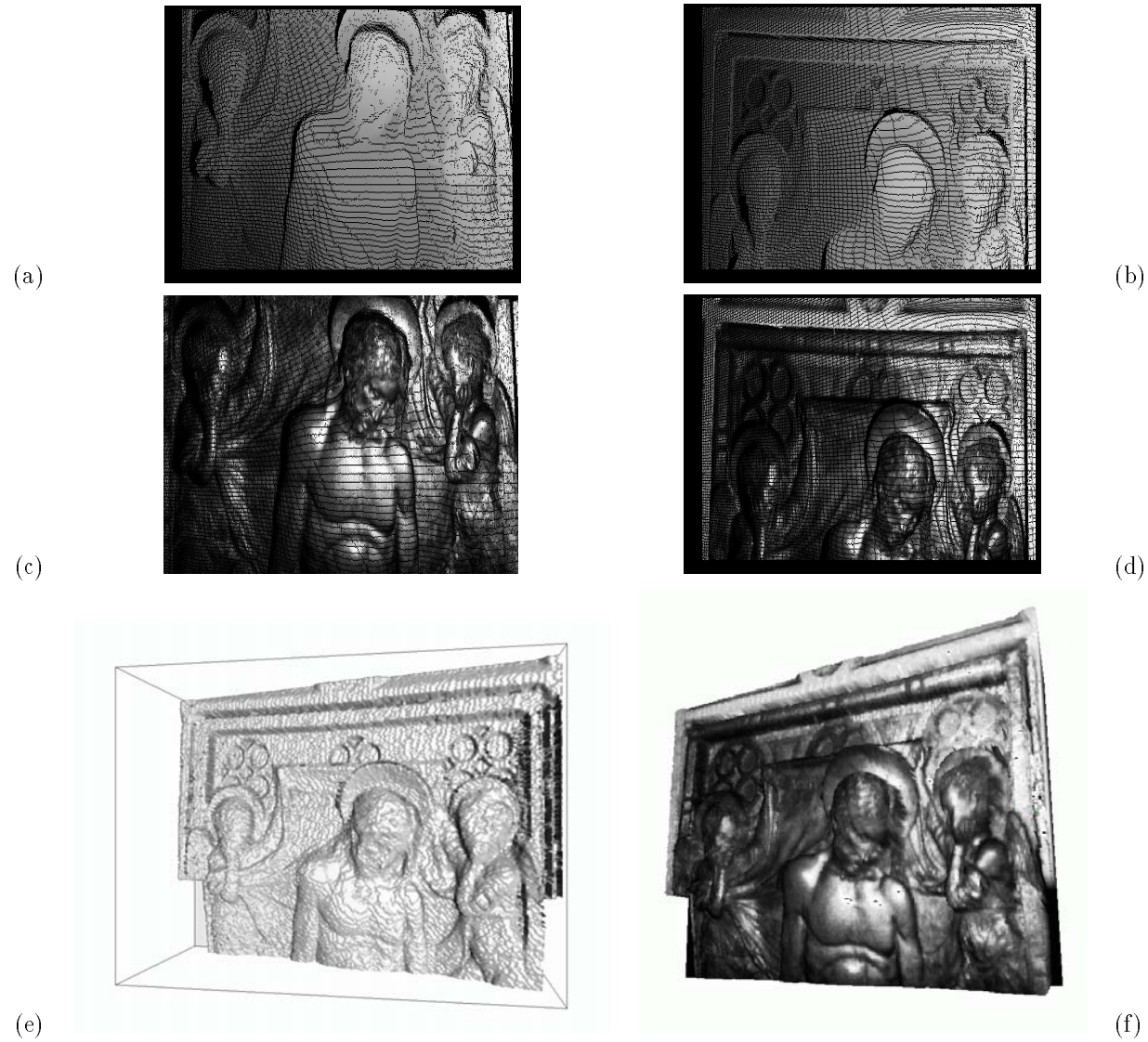

Figure 2: (a), (b) Views of partial range images; (c), (d) textures associated with them; (e) view of the composition of the range data (a), (b); (e) view of the composition of the range and texture data (a), (b), (c), (d).

Step 2′) prescribbes for each pair (k_φ, k_θ) to consider planes at constant k_ρ, and , for each plane, to search for the minimum of functions $\overline{\mathcal{Q}}'$ on a 3×3 window centered at $(k_\rho, k_\varphi, k_\theta)$ and denoted as $W(k_\rho, k_\varphi, k_\theta)$. All the minima found in windows $W(k_\rho, k_\varphi, k_\theta)$ and corresponding to a specific value of k_ρ must be subsequently added together in order to form function $\mathcal{P}'(k_\varphi, k_\theta)$. Function $\mathcal{P}'(k_\varphi, k_\theta)$ is less sensitive to the finite geometry effects plaguing $\mathcal{P}(k_\varphi, k_\theta)$ since $\mathcal{P}'(k_\varphi, k_\theta)$, because of its construction, is able to track the minima of $\overline{\mathcal{Q}}'$ also when they "move" around pixels associated to a specific k_φ value because of quantization effects. The minima of $\mathcal{P}'(k_\varphi, k_\theta)$ computed by 3′) are generally more robust estimates of the rotational axis ω, than those obtained from $\mathcal{P}(k_\varphi, k_\theta)$ by by (8).

3.2 Estimate of the rotational angle ψ

The procedure to determine the rotational angle ψ around rotational axis ω has the followig steps:

1) transform $\mathcal{L}_i, i = 1, 2$ in a cilindrical coordinate system (u, v, w) with the w-axis along ω. In this new reference system the 3-D rotation matrix $R_w(\psi)$ clearly shows the structure of a 2-D rotation by ψ around the w-axis, i.e., it becomes

$$R_w(\psi) = \begin{bmatrix} \cos\psi & -\sin\psi & 0 \\ \sin\psi & \cos\psi & 0 \\ 0 & 0 & 1 \end{bmatrix} \doteq \left[\begin{array}{cc|c} & & 0 \\ & r(\psi) & 0 \\ \hline 0 & 0 & 1 \end{array}\right]; \tag{11}$$

2) project $\mathcal{L}_i$ along the w-axis as

$$p'_i(u,v) = \int_{-\infty}^{+\infty} |\mathcal{L}_i(u,v,w)|\, dw\,, \qquad i = 1,2\,; \tag{12}$$

3) since it is

$$p'_2\left(\left[\begin{array}{c} u \\ v \end{array}\right]\right) = p'_1\left(r^{-1}(\psi)\left[\begin{array}{c} u \\ v \end{array}\right]\right)\,; \tag{13}$$

determine ψ from (13) by the 2-D technique of [5].

The disambiguation between the two admissible estimates $\widehat{\psi}$ and $\widehat{\psi}+\pi$, due to the hermitian symmetry of the Fourier transform, can be accomplished along with the estimate of the translational vector $\mathbf{t}$ (see [6]) by the procedure of section 2.3 of [4].

Since the information about rotation is associated to the low-frequency energy, it was found advisable, instead of using $p'_i(u,v)$ defined by (12) to use their low-passed versions retaining approximately the 20% of the low-frequency energy.

4 EXPERIMENTAL RESULTS

As a practical example of the method, Fig.2-(a) and Fig.2-(b) show two views of two partially overlapped range images of a bas-reliev by the Renaissance sculptor Donatello, belonging to the main altar of the Church of Sant'Antonio in Padova, Fig.2-(c) and Fig.2-(d) shows the textures associated with these two range images. This object, whose dimension are approximately 60×100 cm, is very articulated since there are many anatomical details such as faces, arms, hands, etc., in full 3-D reliev.

The regions of the range images associated to the same scene were determined by a manual procedure and the proposed algorithm was used in order to determine the rotation and the translation between the taking positions of the range camera. Fig.2-(e) shows a view of the 3-D model obtained from the composition of the range images of Fig.2-(a) and Fig.2-(b) based on the estimated rotation and translation, after the noise removal provisions described in [4]. Fig.2-(f) shows a view of the 3-D textured model obtained from the range and texture data of Fig.2.

5 CONCLUSIONS

This work presents the application to 3-D view registration of an algorithm for estimating 3-D rotations and translations based on the frequency domain, preliminarily described in [4]: we reported the algorithmic variations to the procedure of [4] suggested by its actual use. Efficient algorithms for computing the M-D FFT can effectively alleviate the computational burden of operating in the frequency domain [8],[9] The presented technique can be applied to 3-D views registration in low-precision tasks targeted to visualization or it can be used in order to obtain effective starting points for standard methods, which, as well-known, can give accurate solutions, once they are properly initiated [3].

Further work is necessary in order to consolidate the robustness and the efficiency of the proposed 3-D registration technique. An important aspect of the method, is that texture information can be used in order to improve the overall range registration quality.

Acknowledgements

This work has been supported in part by "CNR Progetto Finalizzato Beni Culturali 1997/98". We acknowledge J. A. Beraldin of the Information Technology Group of NRCC-Ottawa and F. Bernier for the range data used in this work.

References

[1] P.J. Besl and N.D. McKay, "A Method for Registration of 3-D Shapes", *IEEE Trans. on PAMI*, Vol. 14, No.2, pp. 239-259, Feb. 1992.

[2] R. Benjemaa, F. Schmitt, "Fast Global Registration of 3-D Sampled Surfaces Using a Multi-Z-Buffer Technique", *Proc. of International Conference on Recent Advances in 3-D Digital Imaging and Modeling*, Ottawa, Canada, May 1997, pp. 113-120.

[3] H. Hügli, C. Schültz, "Geometric Matching of 3-D Objects: Assessing the Range of Successful Initial Configurations", *Proc. of International Conference on Recent Advances in 3-D Digital Imaging and Modeling*, Ottawa, Canada, May 1997, pp. 101-106.

[4] G.M. Cortelazzo, G. Doretto, L. Lucchese, S. Totaro"A Frequency Domain Method for Registration of Range Data", *Proc. of International Symposium on Circuits and Systems*, Monterey, Ca, June 1998.

[5] L. Lucchese, G.M. Cortelazzo, C. Monti, "A Frequency Domain Technique for Estimating Rigid Planar Rotations", *Proc. of International Symposium on Circuits and Systems 96*, Atlanta, Georgia, May 1996, Vol. 2, pp. 774-777.

[6] L. Lucchese, G.M. Cortelazzo and C. Monti, "Estimation of Affine Transformations between Images Pairs via Fourier Transform", *Proc. of IEEE 1996 International Conference on Image Processing*, Lausanne, Switzerland, Sept. 1996, Vol. III, pp. 715-718.

[7] M. Rioux and L. Cournoyer, *The NRCC Three-dimensional Image Data Files*, Ottawa: National Research Council of Canada, June 1988.

[8] R. Bernardini, G.M. Cortelazzo, G.A. Mian, "A Sequential Multidimensional Cooley-Tukey Algorithm", *IEEE Trans. Signal Processing*, 42, pp. 2430-2438, Sept. 1994.

[9] R. Bernardini, G.M. Cortelazzo, G.A. Mian, "Unit Radix Graphs and Their Application to the Computation of MD FFT", submitted.